Synergy between in situ and altimetry data to observe and study the Northern Current variations (NW Mediterranean Sea).

Alice Carret[1], Florence Birol[1], Claude Estournel[2], Bruno Zakardjian[3] and Pierre Testor[4]

5   [1]LEGOS, Université de Toulouse-CNES-CNRS-IRD, OMP, 14 Av. E. Belin, 31400
Toulouse, France
[2]L.A. Université de Toulouse-CNRS, OMP, 14 Av. E. Belin, 31400 Toulouse, France
[3]Université de Toulon, CNRS/INSU, IRD, Mediterranean Institute of Oceanography (MIO),
UM 110, 83957 La Garde, France
10   [4]LOCEAN, Sorbonne Université-CNRS-IRD-MNHN, Paris, France

Correspondence to: Alice Carret : alice.carret@legos.obs-mip.fr

Abstract

During the last 15 years, substantial progress has been achieved in altimetry data processing, providing now data with enough accuracy to illustrate the potential of these observations for coastal applications. In parallel, new altimetry techniques improve the data quality by reducing the land

20   contamination and by enhancing the signal-to-noise ratio. Satellite altimetry provides ever more robust and accurate measurements ever closer to the coast and resolve ever shorter ocean signals. An important issue is now to learn how to use altimetry data in conjunction with the other coastal observing techniques.

Here, we demonstrate the ability of satellite altimetry to observe part of the Northern Current

25   variability. We cross-compare and combine the currents provided by large data sets of ship-mounted ADCPs, gliders, HF radars and altimetry. We analyze how the different available observing techniques capture the current variability at different time-scales. We also study the coherence/divergence/complementarity of the informations derived from the different instruments considered. Two generation of altimetry missions are used: Jason 2 (nadir Ku-band radar) and

30   SARAL/AltiKa (nadir Ka-band altimetry); their performances are compared.

In terms of mean speed of the Northern Current, a very good spatial continuity and coherence is observed at regional scale, showing the complementarity between all the types of current measurements. In terms of current variability, there is still a good spatial coherence but the amplitude of the seasonal variations is underestimated by ~50% in altimetry, compared to both

gliders and ADCPs, because of a too low spatial resolution. For individual dates this number varies a lot as a function of the distance to the coast and width of the Northern Current. Compared to Jason 2, the SARAL/AltiKa data tend to give estimations of the NC characteristics that are closer to in situ data in a number of cases. Satellite altimetry obviously provides a synoptic view of the

5 Northern Current circulation system and variability which helps to interpret the other current observations. Its regular sampling allows the observation of many features that may be missed by in situ measurements.

1   Introduction

Radar altimeters measure the sea surface height (SSH) variations along the satellite tracks at regular interval time. Providing a large number of continuous and ever more accurate observations of the global oceans since more than 25 years, they have progressively evolved into one of the
5   fundamental instruments for many scientific and operational oceanographic applications (Morrow and Le Traon, 2012). The SARAL mission and its first AltiKa Ka-band frequency radar, launched in 2013, has still improved the performance of satellite altimetry (Bonnefond et al., 2018). With the launch of Sentinel-3A, in February 2016, the altimetry constellation was completed by the first global synthetic aperture radar (SAR, or Delay-Doppler) technique which increases the along-track
10   data resolution. These new altimeters provide enhanced accuracy and reduced noise compared to the conventional nadir-looking pulse limited Ku-band instruments used since the beginning of the altimetry era. In 2021, the SWOT mission, with its SAR interferometer in Ka-band measuring SSH over 120-km wide swaths will be a new step forward.

In coastal ocean areas, where it is particularly important to monitor the sea level variations, directly
15   related to our living environments and marine ecosystems, we expect a lot of advances from these new altimetry techniques. Indeed, conventional satellite altimetry missions have not been designed for the observation of the coastal ocean. The strongest limitation is the modification of the radar echo in the vicinity of land. Coastal altimetry measurements are much more difficult to interpret and need a dedicated processing and specific corrections (Gommenginger et al., 2011; Cipollini et al.,
20   2017). The data resolution is also too low to capture the fine scales of the coastal ocean dynamics. As a consequence, most altimetry data collected in coastal zones over the last 25 years have been discarded in altimetry products and/or unexploited. A lot of efforts has been done during the last 15 years in the altimetry community to overcome these difficulties and substantial progress has been achieved on the data processing side (Roblou et al., 2011; Passaro et al., 2014; Valladeau et al.,
25   2015; Cipollini et al., 2017), starting to provide data with enough accuracy to illustrate the potential of altimetry for coastal applications (Passaro et al., 2016; Birol et al., 2017; Morrow et al., 2017). Moreover, the new altimetry techniques are intrinsically less sensitive to the land contamination. They provide more robust and accurate measurements, ever closer to the coast and resolve ever shorter ocean features. We can easily predict that the use of altimetry in coastal studies (Pascual and
30   Gomis, 2003; Bouffard et al., 2008; Birol et al., 2010; Jébri et al., 2016, 2017) will be largely extended in the next years.

Today, coastal observations are mainly based on in situ instruments and satellite imagery (sea surface temperature and ocean color images). In order to answer to the need for monitoring of

the coastal ocean environment, in situ observing systems gather informations in a growing number of regions. The different techniques are often used in conjunction, measuring different ocean state parameters on different time and spatial scales. Compared to altimetry, their spatial and/or temporal resolution is much more adapted to detect the coastal ocean variability. Nonetheless, in situ

5 observations cover more limited areas and often provide time series that present large gaps. Moreover, satellite imagery is often impacted by clouds and does not provide any direct information on the changes occurring in the water column. The large advantage of satellite altimetry, and the reason of its success in the deep ocean, is that it offers almost-global synoptic observations of the sea level, a geophysical parameter which can be related to the ocean circulation and many other

10 dynamical features (eddies, waves, sea water changes, ...). An important issue is now to learn how to use altimetric data in conjunction with the other coastal observing techniques.

To study the contribution of altimetry amongst other types of coastal ocean measurements, the North-Western Mediterranean Sea (NWMed) represents an ideal area. With a Rossby radius of ~10 km, it is associated to important mesoscale and sub-mesoscale variability at all time scales,

15 representing a challenge for observing systems. The main feature of the surface ocean circulation is the Northern Current (called NC hereafter) which is formed in the Ligurian Sea (Taupier-Letage and Millot, 1986) and flows cyclonically along the Italian, French and Spanish coasts. This current presents a marked seasonal variability, with a maximum amplitude from February to April (Sammari et al., 1995; Millot, 1991), and it meanders in a vast range of wavelengths (10-100 km).

20 The mesoscale variability is higher in autumn and winter (Alberola et al., 1995; Millot, 1991). During the last 10 years, the NC has been intensively monitored by a variety of in situ data (moorings, research vessels, gliders, and HF radars) collected from the MOOSE integrated observing system (Mediterranean Ocean Observing System for the Environment). Despite a width of only 30-50 km, through the comparison with ADCP current data, Birol et al., 2010 demonstrated

25 that reprocessed altimetry data are able to partially capture the seasonal variability of the NC and to provide original aspects of the regional circulation. In the Balearic sub-basin, Bouffard et al., 2010, Pascual et al., 2015 and Troupin et al., 2015 showed that coherent circulation patterns could be obtained from altimetry data, in comparison with glider and HF radar data. Morrow et al., 2017 also found similarities between currents measured by gliders and surface currents derived from the most

30 recent altimetry missions.

The general objective of this paper is to demonstrate the ability of satellite altimetry to observe and understand the NWMed ocean dynamics, and to define its contribution compared to the other coastal ocean observing systems. In this study, we combine all the different available in situ data sets which provide information on currents in the Ligurian Sea (ship-mounted ADCPs, gliders and

35 HF radars) and perform systematic comparisons with currents derived from altimetry at different

time-scales. In particular, we analyze how the different available observing techniques capture the NC variability and the coherence/divergence/complementarity of the informations derived. From previous studies, we know that only a small part of the NC variations can be captured by conventional satellite altimetry. Here, we use both Jason-2 and SARAL/AltiKa missions to

5 investigate the progress made from Ku-band to Ka-band altimetry.

In this paper, Sect. 2 presents the datasets used and the corresponding data processing. It is followed by the intercomparison between the currents derived from altimetry and from the different in situ datasets, with the analysis of the NC variations observed at different time scales by the different instruments (Sect. 3). Section 4 concludes the paper.

2 Data and methodology

2.1 Satellite Altimetry

In this study, we use two altimetry missions with distinct characteristics: Jason 2 and SARAL/AltiKA. Jason 2 was launched in June 2008 and provides long time series of data with a

15 10-day repeat observation cycle. The performance of SARAL is significantly better but the corresponding time series started only in February 2013 and have a 35-day repeat observation cycle, a priori not really adapted to the monitoring of the coastal ocean variability. On the other hand, SARAL orbit leads to a smaller distance between tracks, compared to Jason-2 (Fig. 1). Here we focus only on the SARAL tracks 302, 343 and 887 and on the Jason 2 track 222, providing the

20 closest data from the in situ observations.

For both missions, we used the X-TRACK regional product from the CTOH (doi: 10.6096/CTOH_X-TRACK_2017_02), processed with a coastal-oriented strategy (Birol et al., 2017). It consists in time series of Sea Level Anomalies (SLA) every 6-7 km along the satellite tracks, available from 20/07/2008 to 01/10/2016 for Jason 2 (i.e. 300 cycles) and from 24/03/2013

25 to 12/06/2016 for SARAL (i.e. 34 cycles). Considering the data availability (see below for the in situ observations), the study period chosen is 2010-2016.

Jason 2 altimeter is designed as « conventional altimetry » as it operates in the Ku-band frequency. SARAL altimeter operates in the Ka-band, allowing a better performance in terms of spatial resolution (the radar footprint is smaller) and measurement noise. Morrow et al. (2017) analyzed the

30 "mesoscale capability" (defined as the wavelength where the noise is larger than the signal, which varies spatially as shown by Dufau et al., 2016) of these two altimeters in the NWMed using a statistical method (Xu and Fu, 2012). It allows to have an estimate of the size of the structures which can be theoretically detected by each altimeter (in average) and to define the optimal data

spatial filtering. Here, we did the same computation for each of the 4 tracks used in this study, using all the data available (in Morrow et al., 2017, the data located over the continental shelf were discarded). We obtained 49 km for the SARAL track 302, 39 km for the SARAL track 343, 34 km for the SARAL track 887 and 67 km for the Jason 2 track 222, which is coherent with the results of

5 Morrow et al., (2017) who obtained 39 km for SARAL and 55 km for Jason-2 without the coastal altimetry observations. It suggests that the quality of near-shore altimetry SLA remains good.

In order to have the best signal-over-noise ratio, we then filtered the data with a low-pass Loess filter, using a cut-off frequency of 35 km for SARAL. For Jason-2, we chose the option of using a processing as close as possible from the one of SARAL and then used a cut-off frequency of 40 km.

10 One need then to keep in mind that noise remains in the filtered Jason 2 data.

Altimetry only provides sea level anomalies relative to a temporal mean. In order to be able to compare the currents derived from these data with the currents measured or derived from the other instruments (see below), we added the regional Mean Dynamic Topography (MDT) from (Rio et al., 2014) to the altimetric SLA and computed the surface velocities (u) from the total sea level

15 gradients observed between consecutive points along the track, assuming that the fluid is in geostrophic balance:

$$u = \frac{-g}{f} \frac{\triangle (SLA + MDT)}{\triangle x} \quad \text{, where:} \tag{1}$$

f is the Coriolis parameter, g the gravitational constant and $\triangle x$ the distance between the points.

20 ## 2.2 In situ measurements

2.2.1 Glider data

Gliders have been deployed in the NWMed since 2005. However, it is only since 2009 that they are regularly operating as part of the MOOSE network (http://www.moose-network.fr/?page_id=272). In particular, on the Nice-Calvi line (Fig. 1, pink line), 36 deployments were undertaken between

25 2009 and 2016. Some of them have already been analyzed in different studies, with different scientific objectives (Piterbarg et al., 2014 focused on the frontal variability, Bosse et al., 2015 investigated the submesoscale anticyclones, Niewiadomska et al., 2008 analyzed physical-biogeochemical coupling mechanisms). Each glider deployment encompassing several transects, the database includes 204 sections; 192 of them are between 2010 and 2016. The ones being too short

30 or moving too far away from an average trajectory computed from the individual ones were discarded. Finally, 173 glider transects along this line were used in this study. It represents a huge

amount of observations and a large potential of comparisons with altimetry or other in situ observations.

The campaigns were sliced into ascending (from Calvi to Nice) and descending (from Nice to Calvi) transects and the data were projected on a reference track. We assume that one dive or one

5 ascent represents one vertical profile. In practice, data were discarded when the latitude was not monotonically varying or when the angular deviation between 2 consecutive points and the was too strong (larger than 3 standard deviations away from a mean angle). Then the data were gridded with a 4 km horizontal bin size along the reference track (4 km corresponds to the average distance between two successive profiles).

10 During their mission, gliders measure temperature and salinity (among other parameters) from the surface down to 1000 meters (or less if the bottom is shallower, or if commanded to dive shallower). To avoid noise (mainly due to aliased internal waves), temperature and salinity data have to be filtered. A butterworth filter of the second order (Durand et al., 2017) was applied. Different cut-off frequencies have been tested and we finally chose 15 km to avoid noise without

15 removing small-scale variations (as in Bosse et al., 2017). From the temperature and salinity we computed the density and then the geostrophic velocity component perpendicular to the reference track using the thermal wind equation. These velocities are referenced to 500m, corresponding to the depth reached by all gliders.

20 2.2.2 ADCP data

Since 1997, the TETHYS II RV collected a large number of ADCP current measurements during frequent repeated cruises between the French coast (Nice) and the Dyfamed/Boussole site (43°25 N ; 7°52E). The corresponding ship transect is much shorter than the Nice-Calvi glider line (Fig. 1), but samples the NC at about the same location. From 1997 to 2014 a 150 kHz ADCP was used, with

25 a vertical bin length of 4m. In 2015, it was replaced by a 75 kHz ADCP, providing data with a 8 m vertical resolution. The first valid measurement is located at 8/18 m depth for the first/second ADCP. Processed and validated data were obtained from the INSU-DT data center (http://www.dt.insu.cnrs.fr/spip.php?article35). A total of 513 vertical sections of horizontal currents in earth geographical coordinates are provided from November 1997 to March 2017. This number is

30 reduced to 218 during the period 2010-2016. We only used the ADCP transects with a very precise heading which leaves us with 151 sections. Following the same strategy as for glider data, the data were gridded with a 2 km horizontal bin size along a reference transect (from the French coast to DYFAMED site, yellow line on Fig. 1). Ship tracks located outside the chosen grid bins, incomplete transects, as well as data associated to a ship direction which deviates too much from the reference

trajectory (generally corresponding to ship stations) were eliminated. For each cruise, we have one return trip (sometimes two). After a visual inspection of each individual transect to check the coherence of the currents measured during the same day, the data have been averaged per bin, to have one daily-averaged transect. It finally leads to a total of 134 selected current sections. In this

5 study, we focused on the 34m-depth cell, as it is less influenced by surface instrumental errors.

2.2.3   HF radars

The HF radars are also part of the MOOSE network (http://www.moose-network.fr/?page_id=270). The site (indicated in green on Fig. 1) has been chosen to monitor the coastal circulation. There, the

10 bathymetry is very sharp and islands deviate a stronger NC southward. As a consequence, its position and intensity become highly variable, depending on seasonal and wind conditions (Guihou et al., 2013). The system consists in 2 Wellen Radar (WERA) instruments installed near Toulon to monitor seasonal and high frequency variability of the NC. They provide hourly surface current observations. Inertial currents have been filtered. We used edited and daily averaged data provided

15 by MOOSE. The time series starts in May 2012 and ends in September 2014. Due to gaps, only 732 days of data are available.

The size of the area covered by the HF radar is roughly 60x40 km and it is located about 170 km westward of the glider and ADCP observations (as well as of the altimetry tracks we have chosen to focus on in this study).

2.2.d)   Differences between the currents derived from the different observational techniques

In this study, we extensively compare the currents derived from the four different techniques described above with the objective to better understand how they can optimally complement each other for the observation and study of the variability of the NC circulation system. However, we

25 must first have in mind the intrinsic characteristics of each type of current observation and the differences between the data sets.

-   Spatial and temporal sampling

First, the locations of the different types of observations do not coincide with each other, and their temporal and spatial sampling is also very different. After processing, current values are obtained

30 every 2 km along the ship ADCP track, every 4 km along the glider line, in a 3 km resolution grid for the HF radar and every 5-6 km / 7-8 km for Jason 2 / SARAL altimetry, respectively. Moreover, each instrument is characterized by specific measurement errors (and then specific signal to noise ratio) and a filtering has to be applied on the glider and altimetry data, still limiting the wavelengths

of the current which can be resolved (see above and in Table 1). We have also to keep in mind instrumental limitations concerning the area which can be monitored. The ship ADCPs, the HF radars and the gliders have a higher spatial resolution than altimetry but a much more limited spatial coverage. We have also to consider that the access to altimetry data still remains limited in the 10-

5   15 km coastal band. As the NC fluctuates in both location and width (and at both seasonal and much higher frequencies as shown by Albérola et al., 1995), it can make a large difference in the ability of the instrument considered to capture this current flowing along the continental slope, often located very close to the coastline (Fig. 2).

Concerning the temporal sampling, the HF radars and the altimetry provide current observations at

10   regular interval: every day for the HF radar product used here, every 10 days for Jason 2 and every 35 days for SARAL. The glider and ADCP data are available between 0 and 9 times per month and between 0 and 5 times per month, respectively. These unevenly spaced time series make the corresponding data analysis more complex since it can produce significant biases in the distribution of the NC properties (as for example its seasonal variations, see Table 2). It will also be influenced

15   by the period of observations available: from about 2 years for the HF radar to more than 6 years for the ADCP, glider and Jason-2 data (see Table 1).

- **Vertical sampling**

The depth of the current measurement also varies for the different instruments: HF radars and altimeters observe the ocean surface when ADCP and gliders provide vertical sections of

20   measurements. Using both the glider and the ADCP data, we compared the currents computed at different depths (18, 34 and 50 m) and did not find significant differences (less than 5 cm/s for the mean NC core velocity and around 2-3 cm/s for the corresponding STD value). We then decided to use the glider data at 34 m depth (to be coherent with the ADCP observations) and consider that it should not be a significant source of differences with altimetry currents, located at the surface.

25   - **Physical content**

Moreover, the different instruments do not capture the same physical content. The ADCP and the HF radars measure both the total instantaneous velocities when the gliders and altimeters allow to derive only the geostrophic current component perpendicular to the satellite or glider track (i.e. excluding the ageostrophic parts such as wind-driven surface current, tidal currents, internal waves,

30   etc…, and the current component parallel to the track). Unlike the other current data sources used here, altimetry gives only access to current anomalies. But the addition of a synthetic MDT allows to overcome this difficulty if its quality is good enough to derive a reliable mean velocity field. After the addition of the MDT, the gliders and altimeters are clearly the closest in terms of current information derived. However, the glider currents are computed from hydrographic measurement

profiles with a reference level of 500 m (missing the deeper current component), when altimetry currents are derived from sea level measurements (representative of the horizontal density gradients integrated over the whole water column). In this study, in order to minimize (as far as possible) the differences between the current data sets, we performed a projection of the ADCP velocities to

5   obtain the current component perpendicular to the ship transects. Concerning the glider data, estimates of depth-average currents were added to the geostrophic velocities (computed by comparing dead reckoning navigation and GPS fixes at the surface between two surfacing, see Testor et al., 2018 for further information).

All the differences mentioned above are summarized in Table 1. If the data appear complementary

10   in terms of space-time coverage and resolution, we can anticipate that their respective characteristics make their comparison and combination an issue. It is what will be analyzed in details in Sect. 3.

3   Results

3.1   Mean flow and spatial variability: a regional view

From Fig. 1, we can expect that the different observations mentioned above allow to efficiently detect different characteristics of the NC (intensity, position) along its axis, and the variability of

20   these characteristics. In order to have a first general view of how the different velocity fields compare, we have computed their time-average and their standard deviation values at each point of observation for a common period of time: from March 2013 to October 2014. We need to keep in mind that it corresponds to very different sample sizes: 33 ADCP sections, 8 glider transects, 484 days of HF radar measurements and 54-56 and 16 current data for Jason 2 and SARAL satellite

25   altimetry, respectively. Glider / HF radar observations will then have the lowest / highest significance in terms of statistics. Figure 2 shows the resulting map of the mean current and its standard deviation is in Fig. 3. Here, we choose to not represent the results for all the SARAL tracks in order to not overload the figures. Both the regional map (Fig. 2a and 3a) and a zoom in the northern Ligurian Sea (Fig. 2b and 3b), where the largest number of current observations are

30   located, are shown.

Current values are positive (negative) to the right (left) of the ship, glider or satellite tracks (when oriented to the north). Therefore, from Fig. 1 (see the circulation scheme), we expect negative (positive) current values along the northern (southern) branch of the cyclonic NC current system. It

corresponds to what is observed in Fig. 2, where one can notice a very good consistency of the mean currents derived from all the different instruments. Putting together all the pieces of information, the regional structure of the circulation emerges. As already shown in Birol et al. (2010), in the Tyrrhenian Sea, the northwestward Tyrrhenian Current (TC) is well observed at the

5   northern end of Jason 2 track 161. Further north, the NC is formed by the merging of the Eastern Corsica Current (ECC), captured just east of Corsica by the Jason 2 track 085, and of the Western Corsica Current (WCC), well captured by both the gliders and the SARAL track 343. The WCC appears however more extended towards the open sea in the SARAL data, compared to the glider. The NC is then strongly constrained by the bathymetry and follows the continental slope along the

10 coasts of Italy, France and Spain. It can be continuously followed from the SARAL track 343 to the Jason 2 track 070, through the ADCP, glider and HF radar observations. Mean NC velocities larger than -0.3 m/s are observed in the Ligurian Sea (by ADCPs, and altimetry) and off Toulon (by the HF radars and altimetry). Then the continental slope current slows down offshore the Gulf of Lion (the Jason 2 track 146 gives a mean current value of ~-0.15 m/s) and its flow is almost divided by

15 three in the Balearic Sea (~-0.10 m/s). Further south, around 40.5°N around 5-6°E and then between 42°N and 42.5°N around 7-8°E, an eastward flow, probably associated to the Balearic Front which closes the cyclonic circulation south of the Northwestern Mediterranean basin, is captured by the Jason 2 tracks 146, 009, 222 and the SARAL tracks 302 and 887 (from west to east). Around 8°E, it slightly deviates to the southeast before joining the WCC.

20 If we focus on the northern Ligurian Sea (Fig. 2b), the cross-track direction of Jason 2 track 009 is not well oriented compared to the local axis of the NC. In this area, the continental shelf is very narrow and as a consequence the NC is very close to the coast: altimetry struggles to observe the corresponding flow. However, the Jason 2 track 009 and SARAL track 887 still capture a westward current at their northern end. Considering altimetry, Jason 2 track 222, located further

25 southwestward, appears better oriented to monitor the NC. In this area, despite the difference in the number of data samples, the altimetry, ADCP and glider mean current values are very close (between -0,24 and -0,32 m/s for all of them). The width of the NC tends to vary from one instrument to the other. With the gliders it appears slightly narrower than with the ADCP and altimetry (i.e. SARAL track 887). Note also that the ADCPs and gliders, which provide more

30 nearshore information, show a positive or almost null flow very close to the coast, not observed by altimetry (which stop further offshore). Still further West, the altimetry and HF radars also capture a coherent mean NC flow, but with larger values in HF radars (~-0.44 m/s) than in altimetry (~-0.29 m/s).

Figure 3 represents the associated current variability, as captured by the different types of
35 observations. Not surprisingly, in all datasets, larger standard deviation values generally coincide

with the NC system. In altimetry, we observe values of 0.12-0.2 m/s at the northern ends of the Jason 2 tracks 161, 085, 044, 222, 146 and 070 (the signal at the end of track 146 does not correspond to the NC) and of SARAL tracks 302, 343 and 887. If we focus on Fig. 3b, on Jason 2 track 222, we first see clearly the coastal current variations associated to the NC flow (see also Fig.

5   2b). However, the NC is not fully resolved by altimetry: observations stop at ~10 km from land (the more coastal observations have been discarded during the processing, probably due to large data errors). This is even more true for the Jason 2 track 009 (the last data point available is associated to a large suspicious current value) and the SARAL tracks 887 and 302. We have to keep in mind that in this area, where the narrow NC flow is very close to the coastline (its core is in the range 10-40

10   km from land, Piterbarg et al., 2014), its observation by altimetry is very challenging. In comparison, the ADCP, glider and HF radar data allow to observe the NC current variability much closer to the coast (our datasets stop at 2.5 km, 3.5 km and 3-7 km from land, respectively). But they all differ in the current variance captured. Concerning the ADCPs and gliders, observing the NC at the same location, the ADCPs show larger standard deviation values (~0.13 m/s) almost all

15   along the transect when the gliders show much lower values in the open ocean (~0.05 m/s), increasing on the shelf break to values very close to the ones observed on Jason 2 track 222 (~0.12-0.15 m/s). Further west, the HF radars show the largest current variance south of Toulon, with values around 0.23 m/s located on the continental shelf break. In comparison, the corresponding NC variance captured by the SARAL track 302 is only half of that. Further south, off Corsica, the

20   gliders show very low variability (roughly half of the values corresponding to the NC), indicating a WCC flow which is very stable in time (as shown in Astraldi and Gasparini, 1992).

Considering the intrinsic and important differences between the different current datasets (Sect. 2.2.d), these first statistical results are encouraging. They give a coherent picture of the regional circulation, with, except for the HF radars which capture a faster current flow, about the same NC

25   average velocity values. The NC variability is also clearly captured by the different data sets all along its path, but with significant differences in terms of amplitude. Note that when we recompute the standard deviations using a larger period of time (not shown), ADCP and glider tend to converge toward the same cross-shore profile than the one derived from Jason 2 track 222 (with a maximum which is about 0.03 m/s larger for the in situ observations). We can then conclude that this

30   diagnostic is largely influenced by the number of data samples considered as well as by the period of time covered by the measurements.

In order to better understand the differences in variability captured by the various data sets, we analyze the time-space diagrams of the currents derived from ADCP, HF radar, glider and altimetry data over the period considered (Fig. 4). We focus on the first 60 km off the French coast and,

concerning altimetry, on SARAL tracks 302 and 887 and on Jason 2 track 222. The NC is clearly detected in all data but Fig. 4 displays large variations at different timescales (see also Font et al. 1995; Sammari et al., 1995; Albérola et al., 1995) that make the data temporal sampling resolution a very sensitive question if we want to study this current system. The number of glider transects is

5   low and concentrated in 2013 and the unevenly spaced ADCP sections miss a large number of events (spring 2013, winter and summer 2014 are poorly sampled). The HF radar provides a very good temporal sampling according to the one needed to capture the high-frequency NC current variations but it monitors only its section located in the vicinity of Toulon. Altimetry provides then a good complementary information. Despite its relatively low spatial resolution and the intrinsic

10   difficulties when approaching the land, it detects seasonal changes coherent with the ones observed in the other data sets as well as much shorter period changes. Note that if the SARAL mission capabilities are expected to be particularly adapted for fine-scale oceanography and coastal applications (Verron et al., 2018), in our case study its 35-day period appears to be a strong limitation to monitor the highly fluctuating NC flow. This particular point will be further analysed

15   in Sect. 3.3. In the next section, we concentrate on the seasonal variability observed in the different data sets, as it is known to be the dominant signal of the NC system at regional scale (Alberola et al., 1995; Sammari et al., 1995; Crepon et al., 1982; Birol et al., 2010).

20   **3.2   The seasonal variability of the NC flow captured by the different instruments**

Here we compare the monthly climatology (i.e. the mean value for each month of the year) of the maximum NC current amplitude computed from the different current data sets (ADCP, glider, HF radar and altimetry). This time, we use all the data available during the period 01/01/2010 -

25   31/12/2016 (note that the HF radar data are only available over the period 2012-2014). Concerning altimetry, we consider only Jason 2 since we have 2-4 samples per month for SARAL, which is not enough to compute meaningful statistics (see Table 2). For each data sample available, the current profiles along the Jason 2 track 222, the ADCP and glider reference transects and a meridional HF radar section located at 6.2°E, are analyzed. The maximum NC current amplitude is defined as the

30   average of the first decile of the velocity values for each transect and time (remember that the NC corresponds to negative current values). In altimetry, only a distance spanning 60 km to the coast is considered. The number of data in the first decile varies according to the data set and to the number of data in the section considered (because of the lower resolution, it always corresponds to one point in altimetry). As we can see in Fig. 4d, data gaps exist in Jason 2 for some cycles. When it is

35   larger than 3 points, the corresponding cycle is discarded. We also make sure that the velocities

detected correspond to the NC by adding a criterion on the distance allowed between the data points selected in the first decile. Finally, all the information collected are averaged as a function of month and data set and synthesized in monthly climatologies represented in the Fig. 5a,b. For reasons of clarity, results from in situ data are shown in Fig. 5a and results from altimetry are in Fig. 5b, with

5   the glider ones again because this instrument provides the currents which are the closest to altimetry in terms of physical content. For each month, the standard deviation computed from all the NC amplitude values available is also indicated.

Table 2 lists the temporal distribution of the number of samples included in the calculation as a function of month (in brackets). The data density is much more important than in Sect. 3.1 and the

10   corresponding statistics more robust. It appears relatively stable for Jason 2 altimetry and more heterogeneous for the other observations. The number of in situ data per month is strongly variable (especially for the ADCP and to a lesser extent for the glider) and varies also a lot from one year to the other (24 ADCP transects are available in 2015 and only 7 in 2012 and 2014, when the glider dataset has a large gap in 2014). As a consequence, the results will be only discussed in terms of

15   seasonal tendencies.

In Fig. 5a and b, except altimetry, all the climatologies show a clear and coherent seasonal cycle of the NC amplitude, with a stronger/lower flow in winter/summer. As already seen in the previous section, compared to the other data sets, the HF radars capture a faster NC south of Toulon. Higher NC velocities are expected in this location (Ourmières et al., 2011). The corresponding amplitude of

20   the seasonal variations is 0.32 m/s (with a minimum of -0.34 m/s in August and a maximum of -0.66 m/s in February, values also found by Guihou et al., 2013 in this area). In comparison, further East in the northern Ligurian Sea, the peak-to-peak amplitude of the seasonal cycle is slightly lower for the ADCPs than for the HF radars, and associated to a lower mean flow (with a minimum of ~-0.27 m/s in August and a maximum of -0.54 m/s in January). Note however that the value observed

25   in January may be less robust (or at least poorly representative of a mean monthly situation) since it is computed only with 3 data samples. Concerning the gliders, the peak-to-peak amplitude variation is ~20% lower than for the ADCPs, with a minimum of ~-0.25 m/s in August/September and a maximum of -0.46 m/s in December. Since these instruments measure velocities at very close locations, the differences may be mainly due to ageostrophic currents. The Jason 2 climatology

30   displays significantly different results with a series of maxima (~-0.37 m/s in February and November) and minima (~-0.27 m/s in May and October).

To further analyze these results, considering the dispersion of individual current values for each month (Fig. 5a,b, envelopes around the curves), we observe significantly different date-to-date variability for each month (between 0.03 and 0.15 m/s for the glider and ADCP, between 0.12 m/s

and 0.20 m/s for the HF radar and between 0.07 and 0.016 m/s for altimetry). It indicates that the seasonal NC cycle observed in Fig. 5 is modulated by a strong mesoscale and/or year-to-year variability, and it seems to be especially true during intermediate seasons. The dispersion curve of Jason 2 generally follows the other ones except in July and September, when it shows large peaks of

5   variability. Deeper inspection in the corresponding current data set reveals that it is due to much larger NC amplitudes observed during these months in 2014 and 2015. The corresponding NC current intensifications are clearly observed in Fig. 4d in July and September 2014. Unfortunately, no glider transect is available during these periods (Fig. 4c) and we have only one ADCP section which does not show a NC flow increase (Fig. 4b). However, the HF radar currents (Fig. 4f) tend to

10   support that the NC intensification captured by Jason 2 is realistic and not due to altimetry errors (note that one profile of SARAL track 887 is available in July 2014 and that it observes the same feature, Fig. 4a). Since we did not find evidence of summer NC intensification in the previous years, we decided to recompute the seasonal cycle of the NC amplitude using only the data available during the first 6 year-period of Jason-2 (i.e. 2008-2014). We did the same for the ADCPs

15   and gliders, but very few glider data and no ADCP currents are available before 2010 (HF radar currents have not been considered because of the too short length of the time series). The resulting curves are shown in Fig. 5c and a clear seasonal cycle is now also observed in the climatology derived from Jason 2, with a summer/winter decrease/increase of the NC flow. Note that it is also coherent with the results of Birol et al. (2010) who used a combination of the T/P and Jason-1

20   altimeter missions to obtain a current time series over the 1993-2007 time period. The amplitudes of the seasonal variations computed during this new period of time are now around 0.29 m/s, 0.27 m/s (i.e. close to the ones derived from Fig. 5a) and 0.13 m/s for the ADCP, glider and Jason2 altimetry data, respectively. Fig. 5c highlights that the summer velocities measured by the different instruments are relatively close on average. During winter and especially spring, the differences

25   become significant in both amplitude and phase.

Two physical processes can explain the seasonality of the differences between the different types of current measurements. First, the stronger mesoscale variability associated to the NC during these seasons makes the space and time sampling of the current measurements a critical issue for the study of this current system. Second, the strong Tramontane and Mistral winds are more frequent in

30   winter and are decreasing in amplitude from the Gulf of Lion to the Ligurian Sea. This could explain (i) that the differences between the glider and the ADCP current measurements, very close in location, are more important during winter and spring, when the non geostrophic dynamics (in particular the Ekman flow produced by the strong winds) is expected to be the more important and (ii) the strong currents observed by the HF radar in Toulon. The closest seasonal variations to the

35   ones observed by altimetry are found for the glider. It is not surprising since the currents derived

from this instrument are also the closest in terms of physical content (see Sect. 2.2.d). The amplitude of the seasonal variations of the NC captured by the Jason2 track 222 along the French coast is ~50% of the amplitude captured by the glider (which is a good result if we consider the spatial resolution of altimetry data and the width and very coastal location of this current).

3.3 Individual snapshots

To learn more about the similarities and differences between the currents derived from the different instruments, as well as their causes, we now analyze the observations at particular dates. In order to minimize (as far as possible) the differences due to distances in space and time between observations, we focus here on the region near Nice (i.e. on the ADCP and glider data, as well as on the SARAL track 887 and the Jason 2 track 222), and consider only observations that are close in time. For each day of the 2010-2016 study period, we used a time window for each data set (5 days for Jason 2, 10 days for the glider and ADCP data and 22 days for SARAL) and selected only the dates for which we had the four types of observations available. We obtained 7 cases which are reported in Table 3. The corresponding cross-track currents are shown in Fig. 6 (by season) as a function of the distance to the coast. For each case and each data set, we have computed the maximum NC current amplitude (following the same method than in Sect. 3.2) and the corresponding location (expressed in distance to the coast). The results are provided in Table 4.

Figure 6 highlights very different NC situations. Here, the largest coastal current velocities are observed in spring and not in winter as expected from Sect. 3.2. Case 1 (Fig. 6a), the only one in this season, shows (by far) the strongest NC amplitudes in ADCP and glider data (< -0.6 m/s), associated to a narrow flow located within the 30 km coastal band. It corresponds to a difficult study case for altimetry which is still able to depict the NC, but with a too large current vein which amplitude is less than half of what is observed in the in situ observations. Cases 2 and 4 (Fig. 6b,c) are in summer. The NC is broader and its velocity is around -0.3 m/s in all data sets (except in the glider of case 4, see below). This time, altimetry successfully captures the NC amplitude; the location of its core is also good in case 4 but not in case 2 (it is too far/close to the coast for SARAL/Jason 2). In case 4, altimetry and ADCP currents are very close but, for a reason which is unclear (it may be due to a a NC meander or eddy captured by the glider and not by the other instruments), the glider represents a significant slower flow located further south. Cases 5 and 6 (Fig. 6d,e) correspond both to autumn situations but they highlight very different coastal current patterns. In case 5, the glider and SARAL data (corresponding to the same day) are very coherent: they show a relatively weak NC flow (~-0.2 m/s) which core is ~30 km to the coast. Jason 2 observations (very close in time to SARAL and the glider data) show a larger current located

slightly further south (~6 km). The ADCP represents a NC vein at the same location than in the glider and SARAL but with a much stronger amplitude. It could be due either to the differences in the dates of observations (one week, temporal scale at which meanders develop) or to an important ageostrophic NC component. In case 6, Jason 2 does not provide data close enough to the coast to

5   observe the NC. However, the glider, the ADCP and SARAL data show a broad NC located further offshore than in the other cases (its core is located ~ 40 km offshore in ADCP and glider data). As in case 5, the glider and SARAL data provide NC amplitudes and location that are relatively close and the ADCP data give a larger NC maximum. A particular feature in this autumn situation is the succession of very strong and narrow southwestward and then northeastward flows observed in the

10   first 20 km coastal band in both ADCP and glider currents (but not in SARAL which does not get close enough to the coast). It is probably associated to an eddy or meander sticked on the northern anticyclonic side of the NC (eddies were documented at this location in Casella et al., 2011). Finally, cases 3 and 6 (Fig. 6f, g) correspond to winter situations and, as for the autumn, they are very different. In case 3, we observe a broad NC with a core located around 30 km to the coast. The

15   glider exhibit current oscillations along its transect but all current data sets show a coherent representation of the NC, even if the ADCP data provide larger velocities. In case 7, the glider and ADCP capture a narrow NC located ~20 km off the coast also observed by altimetry but with some differences: in Jason 2 the NC flow is slightly broader and in SARAL it is located further offshore. It may be due to rapid variations of the NC between the different dates of observations (12 days

20   between the ADCP and SARAL).

Beyond the large variations of the NC characteristics from one case to the other, an interesting feature in Fig. 6 is the presence of an eastward flow located south of the NC (100-150 km to the coast) in altimetry data in different cases (cases 4, 5 and 6 in particular). The ADCP transect is too short to capture this current vein and it is not observed in the glider data (located further east

25   compared to SARAL track 887 and Jason 2 track 222) which rather depict the WCC on the southern edge of its section. To our knowledge, the corresponding offshore eastward flow is not documented in the literature but its signature seems also be observed in Fig. 2a and 3a (around 42.5°N in SARAL, and around 42.8°N in Jason2). It will be further discussed in the next section.

Finally, what is illustrated in Fig. 6 is that, because of the large short-term changes in the NC

30   circulation system, each snapshot of observations differs significantly from the corresponding seasonal tendency. It highlights the strong interest of long-term and regular altimetry data to study the persistent components of the NC circulation system, as well as its seasonal variations and possible longer-term changes.

3.4 The seasonal variability of the regional surface circulation observed by altimetry

In order to separate the seasonal component of the surface circulation from the mesoscale variations, along each pass of Jason 2 and SARAL located in the area of interest, we have computed a seasonal "climatology" of the cross-track surface geostrophic currents captured by these two altimetry missions (Fig. 7). It was done by simply averaging the corresponding seasonal velocity values for the common 3-year period (April 2013 – April 2016). Note that this type of analysis can be already found in Birol et al. (2010) with a much longer period of altimetry data, but with Jason measurements only (the need to use multi-mission observations was incidentally pointed out in this study). Here, the combination with SARAL data largely improves the spatial resolution of the regional circulation, enabling to capture the main current veins at much more locations along their path (see Fig. 9 of Birol et al., 2010 for comparison).

In Fig. 7, all the structures of the standard circulation scheme of the NW Mediterranean Sea (Fig. 1) are observed: the NC, the WCC, the Balearic Current, the Balearic Front and the TC. What can also be noticed first is the very good coherence and complementarity between the SARAL and Jason 2 climatologies, especially at crossover points (even if differences in the current captured are expected, due to the differences in the track's orientation). The seasonal variations of the regional circulation system already discussed in details in Birol et al. (2010) are confirmed from this different and shorter period of altimetry observations. In particular, if a stronger and unique southwestward flow is observed along the Italian, French and Spanish coasts from autumn to spring, it is not so clear during summer. During this season, the NC does not seem to continue west of 4°E to reach the Balearic Sea. Instead, it may recirculate eastward offshore Cape Creus.

More generally, compared to Birol et al. (2010), the better spatial coverage obtained by combining both SARAL and Jason 2 reveals a circulation scheme that could be much more complex than the one classically proposed in the literature. In summer and autumn (Fig. 8a,d), between 3°E and 9°E, individual eastward current veins are observed between the NC and the Balearic Front, suggesting that recirculations may exist along its path during these seasons. One of them corresponds to the eastward current branch mentioned in Sect. 3.3. Note however that this seasonal analysis is based only on 3 years of observations and could be biased by particular features occuring during 2015. Further investigation based on numerical modeling is clearly needed. This is the next step of this study. But, here again, altimetry appears clearly as a very good tool to first validate the model results.

4   Discussion and conclusion

The characteristics of the dynamics as well as the diverse arrays of in situ instrumentation in the
NWMed offers the possibility to evaluate in details the complementarity between different types of
measurements, including the ones derived from space observations, to monitor the coastal ocean

5   circulation. The NC system in particular is an interesting target since it is a permanent and coherent
current system, associated to a large variability (in both space and time), regularly monitored by a
variety of observation tools. In this study, the systematic comparison of the NC characteristics
(using first statistics, focusing then on seasonal tendencies and finally on individual cases) derived
from the different current data sets provide insights into the causes of their differences as well as

10   into the biases in the NC estimations that these differences may cause.

In this contribution, we have seen that the HF radars provide a good synoptic and daily view of the
NC but only for a small area (60x40 km) and the slope current can be hidden by a strong Ekman
component as they observe only the surface layer. The ship-mounted ADCP permits to see the
vertical NC structure at very high resolution and up to the coast but the measurements may contain

15   unsteady ageostrophic current components such as inertial oscillations (Petrenko et al., 2008). Since
they can be operated on a routine basis only in a few number of places, we have only one regular
section crossing the NC off the French coast (and it is relatively short). It is also the case of gliders
which horizontal resolution and temporal sampling is lower than that of the ADCP and the HF
radars but which provide much longer sections of observations (and also more generally the

20   possibility to measure a large number of physical and biological ocean parameters). Alongtrack
altimetry provides a reasonably good monitoring of surface currents in both space and time but its
spatial resolution does not allow to resolve all the mesoscale and sub-mesoscale signals associated
to the NC.

In this context, the added value of using all these different current measurements in conjunction

25   appears clearly. The present cross-comparison exercise allows to confirm that present day
alongtrack altimetry products provide meaningful estimations of the NC (as already shown in Birol
et al., 2010 and Birol and Delebecque, 2014). If the spatial resolution allowed by satellite altimeters
limits the current component which can be captured, the missing variability can be quantified using
the other current observations. If we consider a reasonably long time series of observations

30   including enough data samples for each instrument (see Sect. 3.2), in the northern Ligurian Sea, the
average NC value derived from altimetry (-0.3m/s) is coherent with the one derived from the other
instruments. But the amplitude of its seasonal variations is underestimated by ~50% compared to
both the glider (closest instrument in terms of physical content of current estimations) and the
ADCP (the highest resolution current data set). It means that in this case the seasonal cycle of the

35   non-geostrophic current component is very low. However, for individual dates this number varies a

lot as a function of the distance to the coast and width of the NC (from a correct NC amplitude estimation to no NC observation) but a quantification of the high frequency component of the coastal ocean dynamics that altimetry is able to capture would require data that are colocalized in both space and time. Compared to Jason 2, the SARAL altimeter data tend to give estimations of the

5   NC characteristics that are closer to in situ data in a number of cases but its 35-day cycle is clearly a strong limitation for the study of this coastal current system. Despite this problem of spatial resolution, altimetry obviously provides a synoptic view of the circulation system and variability which helps to interpret the other current observations as well as analyze their limitations. It also reveals features that are not (to our knowledge) documented in the literature and that are not (or

10   poorly) captured by the currents derived from the other instruments. It is the case of possible NC recirculation branches and of the summer NC increase in 2014 and 2015.

Not surprisingly, one conclusion of this study is that the data resolution and sampling is clearly an issue to capture the large range of frequencies found in the NWMed coastal ocean (and we can easily assume that it is true for many other coastal ocean areas). In particular, the temporal data

15   coverage is a large source of differences between the NC statistics computed from the different observing systems. A second cause of differences in the estimations of the NC characteristics appears to be due to ageostrophic flow, principally the Ekman and inertial currents, measured by the ADCP and HF radars but not represented in the glider (they are partially included through the correction of the depth-average currents) and altimeter-derived geostrophic currents. Clearly, a

20   multi-data combined approach is the unique way to obtain a complete picture of a dynamical system as complex as the NC and altimetry is one component of the observing system needed.

Finally, it is important to note that improved altimetry data processing and corrections as well as technical innovations lead to an ever increasing number of coastal data ever closer to the coastline. It raises the question of the calibration and validation of these new data against independent in situ

25   observations. How can we robustly quantify the evolution of the new processing and products? We benefit from the long experience of nadir altimetry technology, widely based on tide gauges sea level observations taken as an independent reference. However a full understanding and exploitation of the new performances allowed by the Ka-band, SAR and SAR-in altimetry techniques requires new methods and validation means. We advocate that only a combination of in

30   situ instruments providing regular cross-shore informations along altimetry tracks will allow to understand and exploit the full capability of altimetry in coastal observing systems and guide its evolution. Beyond the case study presented here, such cross-comparison exercises between altimetry and different types of in situ observing systems allows to identify how they can be combined for advanced altimetry validation purposes.

Acknowledgements*.*

5 This study was done with the financial support of the Region Occitanie and the CNES through their PhD funding programs. The ship-mounted ADCP data were kindly provided by the DT-INSU who did the acquisition, management and processing. Altimetry data used in this study were developed, validated, and distributed by the CTOH/LEGOS, France.Glider data were collected and made freely available by the Coriolis project (http://www.coriolis.eu.org) and programs that contribute. We

10 would like to acknowledge the staff of the French National Pool of Gliders (DT-INSU/CNRS - CETSM/Ifremer) for the sustained gliders deployments carried out in the framework of MOOSE. Support was provided by the French ''Chantier Méditerranée'' MISTRALS program (HyMeX and MERMeX components) and by the EU projects FP7 GROOM (grant agreement 284321), FP7 PERSEUS (grant agreement 287600), FP7 JERICO (grant agreement 262584), and the COST

15 Action ES0904 ''EGO'' (Everyone's Gliding Observatories). HF radar data were funded as part of the French MOOSE Mediterranean observing system program.

References

20 Alberola, C., Millot C., and Font J.: On the seasonal and mesoscale variabilities of the Northern Current during the PRIMO-0 experiment in the western Mediterranean-sea. Oceanol Acta, 18(2), 163–192, 1995

Astraldi, M., and Gasparini G. P.: The seasonal characteristics of the circulation in the north Mediterranean basin and their relationship with the atmospheric-climatic conditions. J Geophys

25 Res-Oceans, 97(C6), 9531–9540, https://doi.org/10.1029/92JC00114. 1992

Birol, F., and Delebecque C.: Using high sampling rate (10/20Hz) altimeter data for the observation of coastal surface currents: A case study over the northwestern Mediterranean Sea. J Marine Syst, 129, 318–333, https://doi.org/10.1016/j.jmarsys.2013.07.009, 2014

Birol, F., Cancet M., and Estournel C.: Aspects of the seasonal variability of the Northern

30 Current (NW Mediterranean Sea) observed by altimetry. J Marine Syst, 81(4), 297–311, https://doi.org/10.1016/j.jmarsys.2010.01.005, 2010

Birol, F., Fuller N., Lyard F., Cancet M., Niño F., Delebecque C., Fleury S., Toublanc F., Melet A., Saraceno M., and Léger F.: Coastal applications from nadir altimetry: Example of the X-TRACK regional products. Adv Space Res, 59(4), 936–953,

35 https://doi.org/10.1016/j.asr.2016.11.005, 2017

Bonnefond P., Verron J., Aublanc J., Babu K. N., Bergé-Nguyen M., Cancet M., Chaudhary A., Créteaux J. F., Frappart F., Haines B. J., Laurain O., Ollivier A., Poisson J. C., Prandi P., Sharma R., Thibaut P., Watson C.: The Benefits of the Ka-Band as Evidenced from the SARAL/AltiKa Altimetric Mission: Quality Assessment and Unique Characteristics of AltiKa Data. Remote

5   Sensing, 10 (83), https://doi.org/10.3390/rs10010083, 2018

Bosse A., Testor P., Mayot N., Prieur L., D'Ortenzio F., Mortier L., Le Goff H., Gourcuff C., Coppola L., Lavigne H., Raimbault P.: A submesoscale coherent vortex in the Ligurian Sea: From dynamical barriers to biological implications. J Geophys Res-Oceans, 122(8), 6196-6217, https://doi.org/10.1002/2016JC012634, 2017

10   Bosse A., Testor P., Mortier L., Prieur L., Taillandier V., d'Ortenzio F., and Coppola L.: Spreading of Levantine Intermediate Waters by submesoscale coherent vortices in the northwestern Mediterranean Sea as observed with gliders. J Geophys Res-Oceans, 120(3), 1599–1622, https://doi.org/10.1002/2014JC010263, 2015

Bouffard J., Pascual A., Ruiz S., Faugère Y., and Tintoré J.: Coastal and mesoscale dynamics

15   characterization using altimetry and gliders: A case study in the Balearic Sea. J Geophys Res-Oceans, 115(C10), C10029, https://doi.org/10.1029/2009JC006087, 2010

Bouffard J., Vignudelli S., Cipollini P., Menard Y.: Exploiting the potential of an improved multimission altimetric data set over the coastal ocean. Geophys Res Lett, 35(10), https://doi.org/10.1029/2008GL033488, 2008

20   Casella, E., Molcard A., and Provenzale A.: Mesoscale vortices in the Ligurian Sea and their effect on coastal upwelling processes. J Marine Syst, 88(1), 12–19, https://doi.org/10.1016/j.jmarsys.2011.02.019, 2011

Cipollini P., Calafat F. M., Jevrejeva S.,Melet A., Prandi P.: Monitoring Sea Level in the Coastal Zone with Satellite Altimetry and Tide Gauges. Surv Geophys, 38(1), 33-57, 2017

25   Crépon M., Wald L., Monget J. M.: Low-frequency waves in the Ligurian Sea during December 1977. J Geophys Res. 87(C1), 595-600. https://doi.org/10.1029/JC087iC01p00595, 1982

Dufau C., Orsztynowicz M., Dibarboure G., Morrow R., Le Traon P. Y.: Mesoscale resolution capability of altimetry: Present and future. J Geophys Res-Oceans, 121(7), 4910-4927 https://doi.org/10.1002/2015JC010904, 2016

30   Durand, F., Marin F., Fuda J.-L., and Terre T.: The East Caledonian Current: A Case Example for the Intercomparison between AltiKa and In Situ Measurements in a Boundary Current. Mar Geod, 40(1), 1–22, https://doi.org/10.1080/01490419.2016.1258375, 2017

Font J., Garcialadona E., Gorriz E. G.: The seasonality of mesoscale motion in the northern current of the western Mediterranean – several years of evidence. Oceanol Acta, 18(2), 207-219,

35   1995

Gommenginger C., Thibaut P., Fenoglio-Marc L., Quartly G., Deng X., Gomez-Enri J., Challenor P., Gao Y.: Retracking Altimeter Waveforms Near the Coasts. Coastal Altimetry, 61-101, 2011

Guihou K., Marmain J., Ourmières Y., Molcard A., Zakardjian B., and Forget P.: A case study of the mesoscale dynamics in the North-Western Mediterranean Sea: a combined data–model approach. Ocean Dynam, 63(7), 793–808, https://doi.org/10.1007/s10236-013-0619-z, 2013

Jébri F., Birol F., Zakardjian B., Bouffard J., Sammari C.: Exploiting coastal altimetry to improve the surface circulation scheme over the central Mediterranean Sea. J Geophys Res-Oceans 121(7), 4888-4909, https://doi.org/10.1002/2016JC011961, 2016

Jébri F., Zakardjian B., Birol F., Bouffard J., Jullion L., Sammari C.: Interannual Variations of Surface Currents and Transports in the Sicily Channel Derived From Coastal Altimetry. J Geophys Res-Oceans 122(11), 8330-8353, https://doi.org/10.1002/2017JC012836, 2017

Millot C.: Mesoscale and seasonal variabilities of the circulation in the western Mediterranean. Dynam Atmos Oceans, 15(3), 179–214, https://doi.org/10.1016/0377-0265(91)90020-G, 1991

Morrow, R., and Le Traon P.-Y.: Recent advances in observing mesoscale ocean dynamics with satellite altimetry. Adv Space Res, 50(8), 1062–1076, https://doi.org/10.1016/j.asr.2011.09.033, 2012

Morrow R., Carret A., Birol F., Nino F., Valladeau G., Boy F., Bachelier C., and Zakardjian B.: Observability of fine-scale ocean dynamics in the northwestern Mediterranean Sea. Ocean Sci, 13(1), 13–29, https://doi.org/10.5194/os-13-13-2017, 2017

Niewiadomska K., Claustre H., Prieur L., and d'Ortenzio F.: Submesoscale physical-biogeochemical coupling across the Ligurian current (northwestern Mediterranean) using a bio-optical glider. Limnol Oceanogr, 53(5), 2210, 2008

Ourmières Y., Zakardjian B., Béranger K., and Langlais C.: Assessment of a NEMO-based downscaling experiment for the North-Western Mediterranean region: Impacts on the Northern Current and comparison with ADCP data and altimetry products. Ocean Model, 39(3–4), 386–404, https://doi.org/10.1016/j.ocemod.2011.06.002, 2011

Pascual A., Lana A., Troupin C., Ruiz S., Faugère Y., Escudier R., and Tintoré J.: Assessing SARAL/AltiKa Data in the Coastal Zone: Comparisons with HF Radar Observations. Mar Geod, 38(sup1), 260–276, https://doi.org/10.1080/01490419.2015.1019656, 2015

Pascual A. and Gomis D.: Use of Surface Data to Estimate Geostrophic Transport. J Atmos Ocean Tech, 20, 912-926, 2003

Passaro M., Cipollini P., Vignudelli S., Quartly G. D., Snaith H. M.: ALES: A multi-mission adaptive subwaveform retracker for coastal and open ocean altimetry. Remote Sens Environ, 145, 173-189, 2014

Passaro M., Dinardo S., Quartly G. D., Snaith H. M., Benveniste J., Cipollini P., Lucas B.: Cross-calibrating ALES Envisat and CryoSat-2 Delay–Doppler: A coastal altimetry study in the Indonesian Seas. Adv Space Res, 58(3), 289-303, http://dx.doi.org/10.1016/j.asr.2016.04.011, 2016

Petrenko A., Dufau C. and Estournel C.: Barotropic eastward currents in the western Gulf of Lion, north-western Mediterranean Sea, during stratified conditions. J Marine Syst, 74(1-2), 406-428, 2008

Piterbarg L., Taillandier V., and Griffa A.: Investigating frontal variability from repeated glider transects in the Ligurian Current (North West Mediterranean Sea). J Marine Syst, 129, 381–395, https://doi.org/10.1016/j.jmarsys.2013.08.003, 2014

Rio M.-H., Pascual A., Poulain P.-M., Menna M., Barceló B., and Tintoré J.: Computation of a new mean dynamic topography for the Mediterranean Sea from model outputs, altimeter measurements and oceanographic in situ data. Ocean Sci, 10(4), 731–744, https://doi.org/10.5194/os-10-731-2014, 2014

Roblou L., Lamouroux J., Bouffard J., Lyard F., Le Hénaff M., Lombard A., Marsaleix P., De Mey P., Birol F.: Post-processing altimeter data towards coastal applications and integration into coastal models. Coastal Altimetry, 217-246, 2011

Sammari C., Millot C., and Prieur L.: Aspects of Seasonal and Mesoscale Variabilities of the Northern Current in the Western Mediterranean-Sea Inferred from the PROLIG-2 and PROS-6 Experiments. Deep-Sea Res Pt I, 42(6), 893–917, https://doi.org/10.1016/0967-0637(95)00031-Z, 1995

Taupier-Letage I., and Millot C.: General hydrodynamical features in the Ligurian Sea inferred from the DYOME experiment. Oceanol Acta, 9(2):119–131, 1986

Testor P., Bosse A., Houpert L., Margirier F., Mortier L., Legoff H., Dausse D., Labaste M., Karstensen J., Hayes D., Olita A., Ribotti A., Schroeder K., Chiggiato J., Onken R., Heslop E., Mourre B., d'Ortenzio F., Mayot N., Lavigne H., de Fommervault O., Coppola L., Prieur L., Taillandier V., De Madron XD., Bourrin F., Many G., Damien P., Estournel C., Marsaleix P., Taupier-Letage I., Raimbault P., Waldman R., Bouin M. N., Giordani H., Caniaux G., Somot S., Ducrocq V., Conan P.: Multiscale observations of deep convection in the northwestern Mediterranean Sea during winter 2012–2013 using multiple platforms. J Geophys Res-Oceans, 123(3), 1745-1776. https://doi.org/10.1002/2016JC012671, 2018

Troupin C., Pascual A., Valladeau G., Pujol I., Lana A., Heslop E., Ruiz S., Torner M., Picot N., and Tintoré J.: Illustration of the emerging capabilities of SARAL/AltiKa in the coastal zone

using a multi-platform approach. Adv Space Res, 55(1), 51–59, https://doi.org/10.1016/j.asr.2014.09.011, 2015

Valladeau G., Thibaut P., Picard B., Poisson J. C., Tran N., Picot N., Guillot A.: Using SARAL/AltiKa to improve Ka-band altimeter measurements for coastal zones, hydrology and ice:

5   The PEACHI prototype. Mar Geod, 38(sup1), 124-142, http://dx.doi.org/10.1080/01490419.2015.1020176, 2015

Verron J., Bonnefond P., Aouf L., Birol F., Bhowmick S. A., Calmant S., Conchy T., Crétaux J.-F., Dibarboure G., Dubey A. K., Faugère Y., Guerreiro K., Gupta P. K., Hamon M., Jebri F., Kumar R., Morrow R., Pascual A., Pujol M. I., Rémy E., Rémy F., Smith W. H. F., Tournadre J., and

10 Vergara O.: The benefits of the Ka-band as evidenced from SARAL/AltiKa altimetric mission. Part 2: scientific applications. Remote Sensing 10(2), 163 https://doi.org/10.3390/rs10020163, 2018

Xu Y., and Fu L.-L.: The Effects of Altimeter Instrument Noise on the Estimation of the Wavenumber Spectrum of Sea Surface Height. J Phys Oceanogr, 42(12), 2229–2233, https://doi.org/10.1175/JPO-D-12-0106.1, 2012

Table 1: Main characteristics of the different current data sets used in this study.

Instrument	Physical content	Depth	Spatial resolution	Temporal resolution	First and last dates in the data record	Number of sections selected	Filtering
HF radars	Absolute surface current	surface	3 km	daily	May 2012 - September 2014	732	No
ADCP	Vertical section of absolute current	34 m chosen for this study	1.3 km	unevenly spaced : 1 day to 6 months between consecutive data	May 2010 - November 2016	134	No
Gliders	Vertical section of geostrophic current (baroclinic component above 1000 m + additional correction)	34 m chosen for this study	4 km	unevenly spaced : 1 day to 1 year between consecutive data	June 2010 - September 2016	173	15 km
Jason 2	Surface geostrophic current	surface	5.75 km	~ 10 days	January 2010 - October 2016	246	40 km
SARAL	Surface geostrophic current	surface	7.38 km	35 days	April 2013 - May 2016	34	35 km

Table 2: Number of data sample per month for each current dataset during the period 01/01/2010 - 31/12/2016. The number of data selected for the climatology computation is indicated in brackets.

Instrument	Jan	Feb	Mar	Apr	May	June	July	Aug	Sep	Oct	Nov	Dec
radars	62 (60)	56 (55)	62 (62)	60 (60)	93 (70)	90 (90)	93 (91)	93 (52)	90 (70)	62 (35)	60 (29)	62 (53)
ADCP	6 (3)	20 (11)	18 (5)	20 (10)	15 (8)	25 (9)	18 (11)	24 (15)	20 (12)	11 (6)	24 (15)	17 (8)
Gliders	6 (6)	20 (20)	12 (10)	12 (12)	10 (10)	28 (23)	26 (22)	14 (14)	10 (9)	17 (15)	17 (14)	20 (16)
Jason 2	22 (19)	20 (20)	21 (20)	20 (18)	21 (21)	21 (20)	22 (21)	22 (21)	20 (17)	19 (19)	18 (17)	19 (19)
Saral	3	3	2	3	4	4	2	2	3	3	3	2

Table 3: List of the cases of relative colocatisation in time between the glider, ADCP and atimetry current data, and corresponding dates of observations.

	Date of observations				
	Glider	ADCP	SARAL altimetry (track 887)	Jason 2 altimetry (track 222)	Temporal window
Case 1 (Fig. 6a): April 2013	11-13/04/2013	11/04/2013	14/04/2013	11/04/2013	4 days
Case 2 (Fig. 6b): July 2013	12-14/07/2013	13/07/2013	28/07/2013	09/07/2013	20 days
Case 3 (Fig. 6g): February 2015	6-15/02/2015	09/02/2015	08/02/2015	04/02/2015	12 days
Case 4 (Fig. 6c): September 2015	18-26/09/2015	22/09/2015	06/09/2015	20/09/2015	21 days
Case 5 (Fig. 6d): October 2015	06-11/10/2015	17/10/2015	11/10/2015	10/10/2015	12 days
Case 6 (Fig. 6e): November 2015	13-21/11/2015	12/11/2015	15/11/2015	18/11/2015	10 days
Case 7 (Fig. 6f): February 2016	1-9/02/2016	05/02/2016	24/01/2016	27/01/2016	17 days

Table 4: Maximum NC current value deduced from the glider, ADCP and atimetry current data for the 7 individual cases listed in Table 3.

| | Maximum NC value and distance to the coast of this maximum | | | |
	Glider	ADCP	Saral altimetry (track 887)	Jason 2 altimetry (track 222)
Case 1	18 km -0.66 m/s	23 km -0.74 m/s	14 km -0.32m/s	13 km -0.28 m/s
Case 2	22 km -0.27 m/s	28 km -0.31 m/s	43 km -0.33 m/s	13 km -0.30 m/s
Case 3	30 km -0.30 m/s	33 km -0.51 m/s	29 km -0.24 m/s	36 km -0.29 m/s
Case 4	42km -0.16 m/s	18 km -0.28 m/s	14 km -0.34 m/s	13 km -0.31 m/s
Case 5	23 km -0.22 m/s	26 km -0.42 m/s	29 km -0.21 m/s	36 km -0.35 m/s
Case 6	30 km -0.25 m/s	40 km -0.34 m/s	29 km -0.21 m/s	no data
Case 7	14 km -0.30 m/s	16 km -0.42 m/s	43 km -0.39 m/s	30 km -0.35 m/s
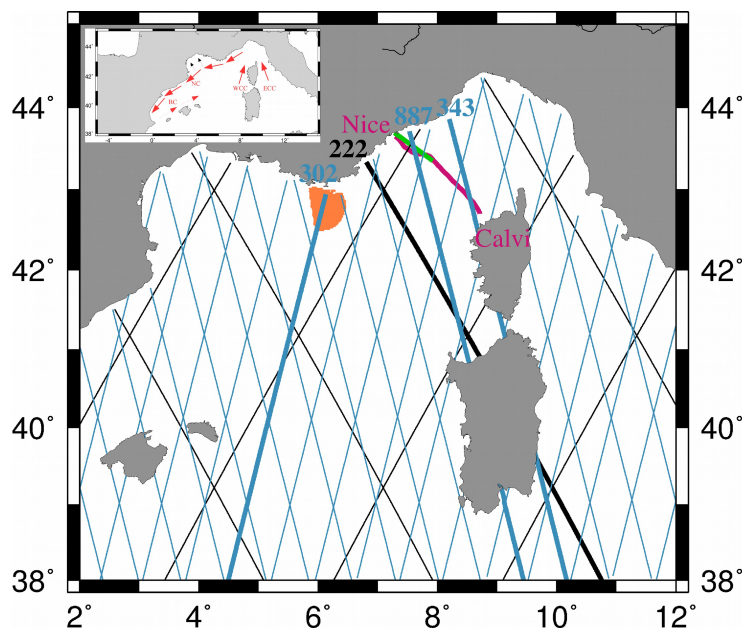
Figure 1: Study area and data distribution. Jason 2 and SARAL tracks are represented by the black and blue lines, respectively. The satellite tracks used in the study are indicated in bold. The region in orange corresponds to the HF radar coverage. The Nice-Calvi glider line is in purple and the Thetys ADCP transect is in green. A map of the schematic regional circulation is presented at the upper left hand corner.
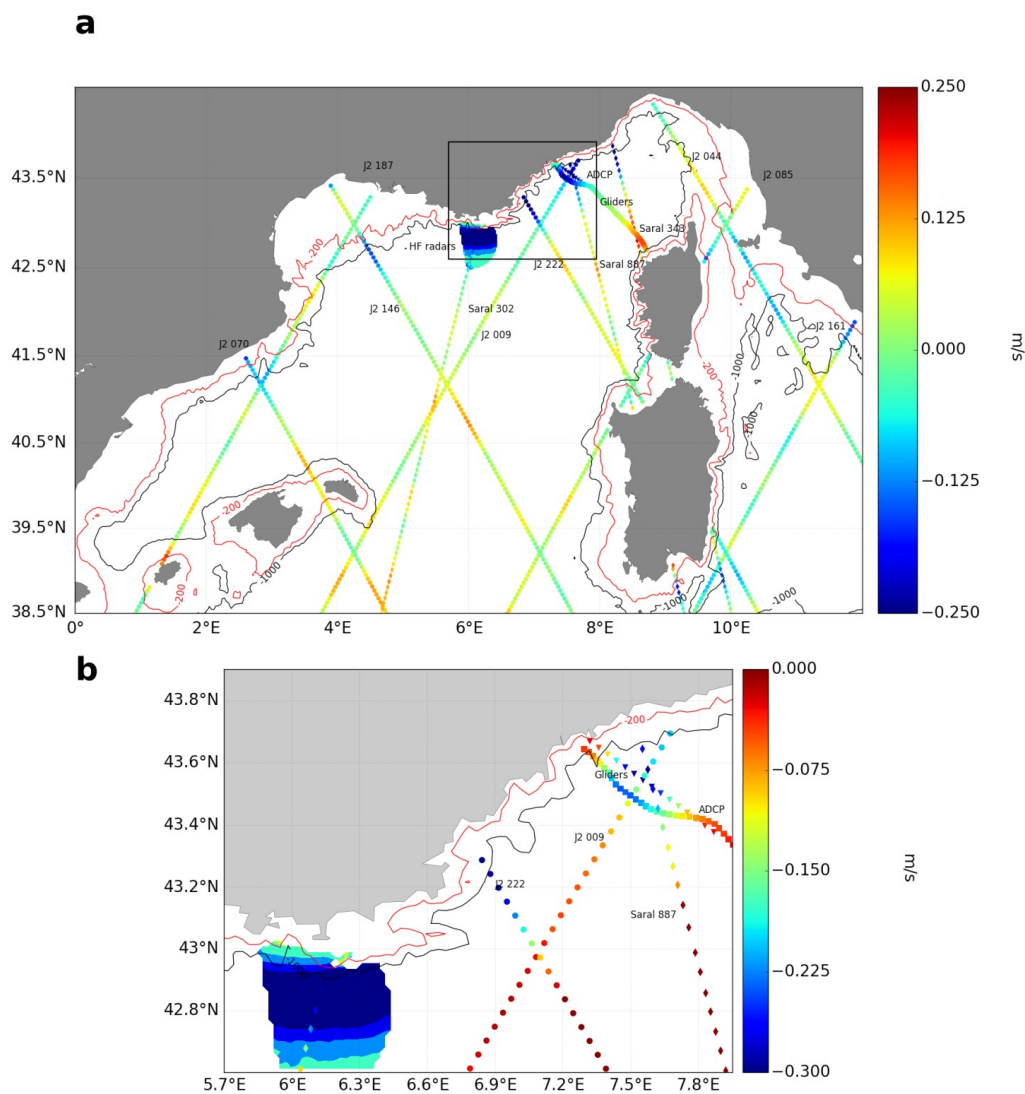
Figure 2: a) Map of the mean current values derived from ADCP, glider, HF radar and altimetry data over the period 03/2013 – 10/2014. b) Zoom in the northern Ligurian Sea (black rectangle indicated in Figure 2a). The 200-m (red line) and 1000-m (black line) are also shown.
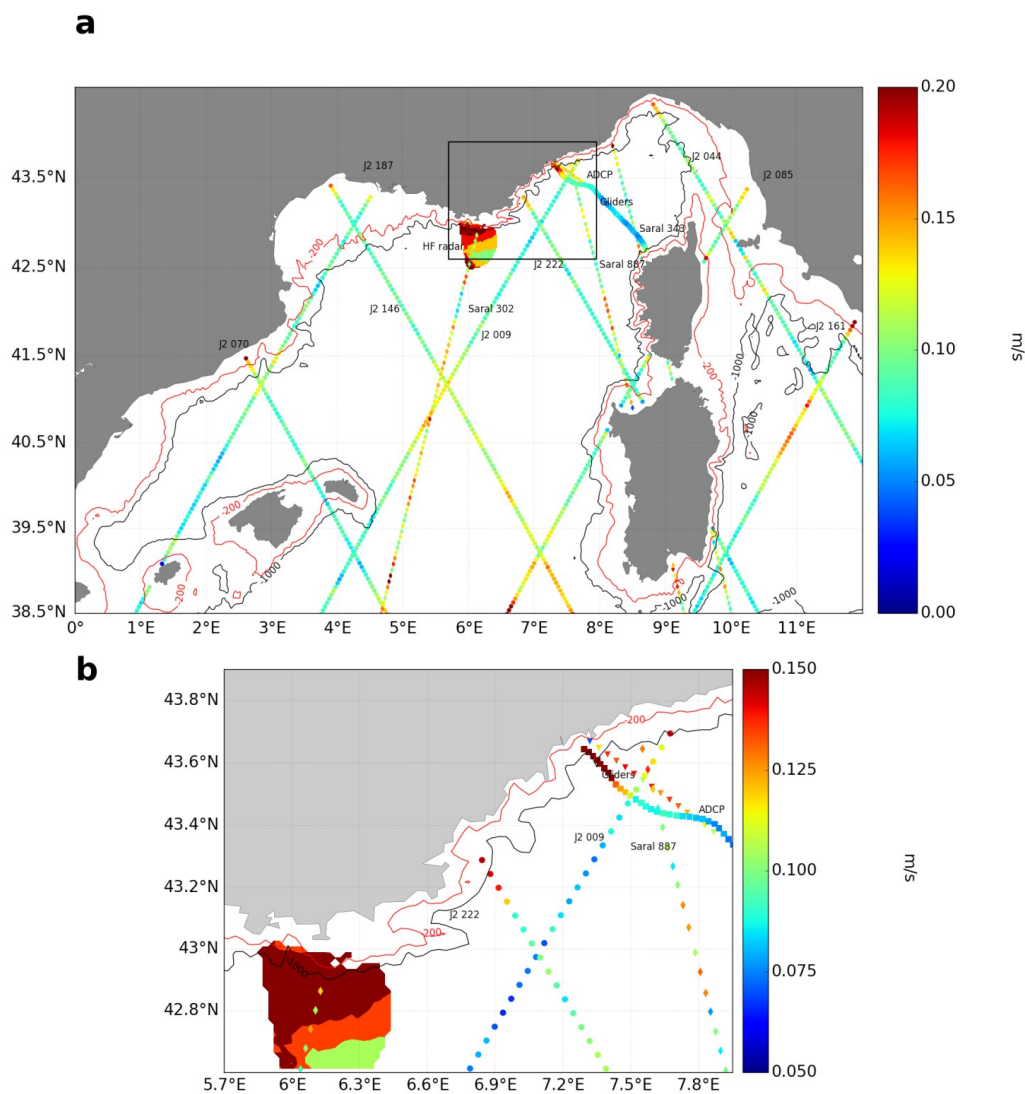
Figure 3: a) Map of the standard deviations of the velocities derived from ADCP, glider, HF radar and altimetry data over the period 03/2013 – 10/2014. b) Zoom in the northern Ligurian Sea (black rectangle indicated in Figure 3a). The 200-m (red line) and 1000-m (black line) are also shown
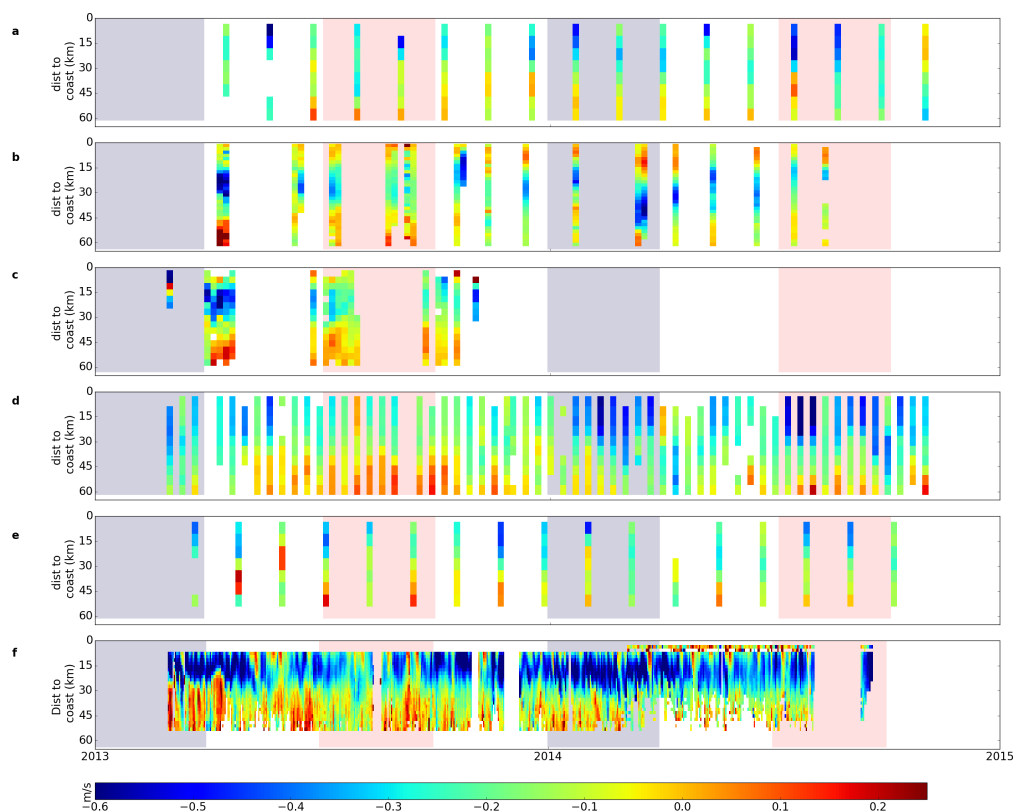
Figure 4: Time-space diagrams of the current velocities derived from a) SARAL track 887 b) ADCP, c) Gliders, d) Jason 2 track 222, e) SARAL track 302 and f) HF radars between March 2013 and October 2014. The pink and purple areas in the background of the diagrams correspond to the summer and winter seasons, respectively.
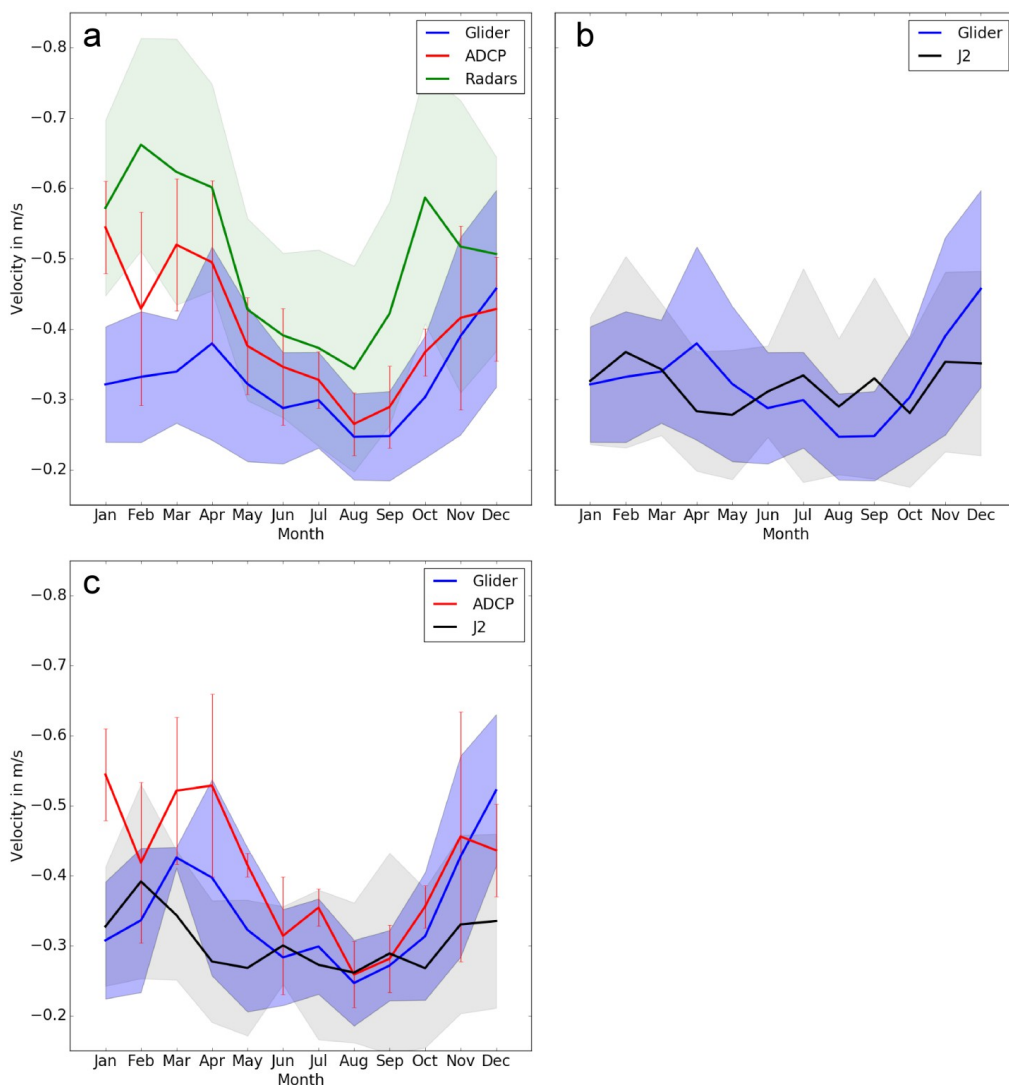
Figure 5: Seasonal variations of the maximum current amplitude derived from the a) HF radars (green line), ADCP (red line), gliders (blue line), and b) Jason 2 (black line) and glider (blue line) observations available over the period 01/01/2010 - 31/12/2016. c) Same than a) and b) but computed over the period July 2008 to June 2014 and only for the gliders, ADCP and Jason 2. For all the curves the monthly standard deviation of the maximum current amplitude derived from the corresponding instrument is also indicated (curve envelopes and error bars).
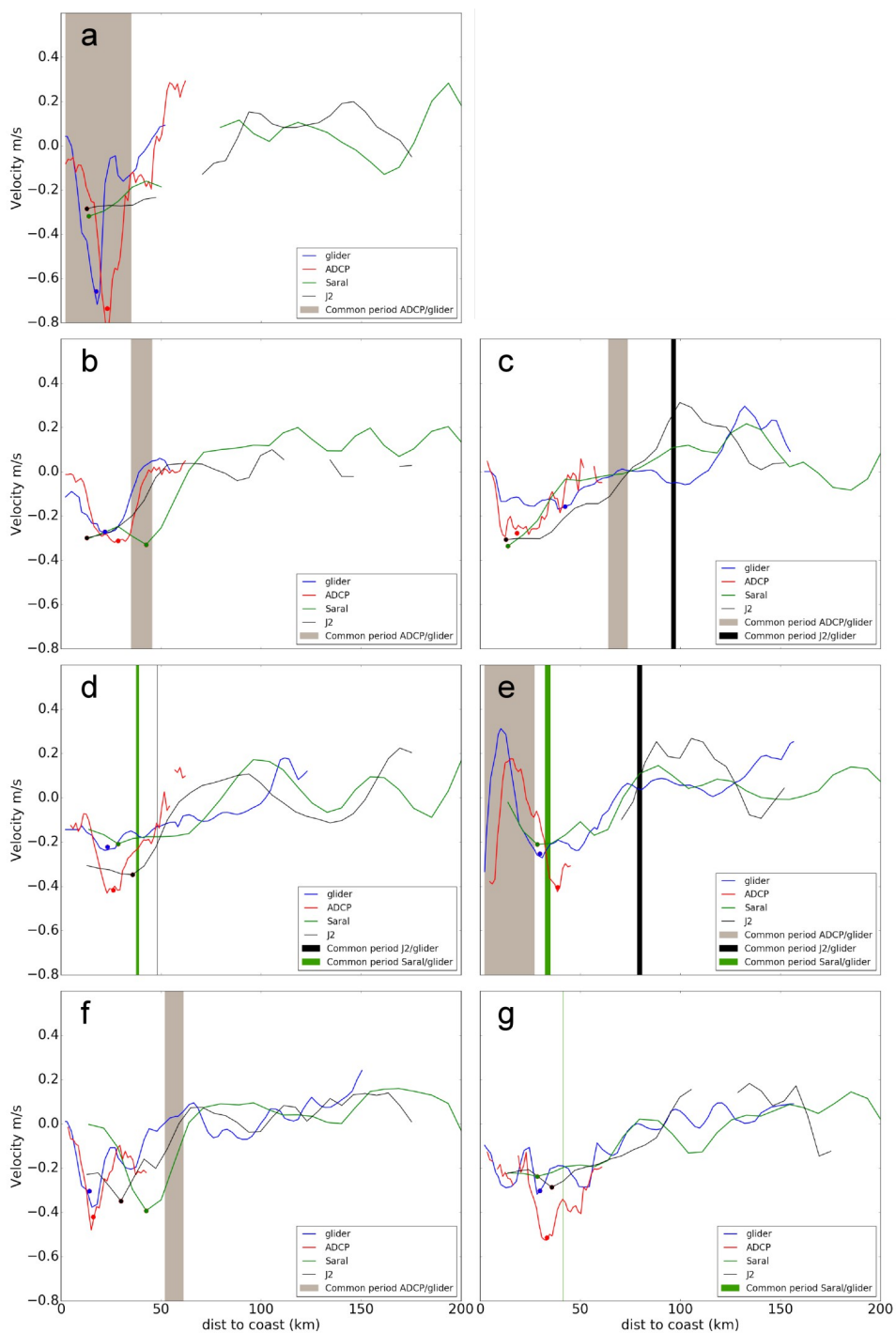
Figure 6: Cross-shore sections of currents deduced from the glider (blue), ADCP (red), SARAL (green) and J2 (black) altimetry data for the 7 individual cases identified in Table 3. Overlapping periods between the different observations are also indicated.
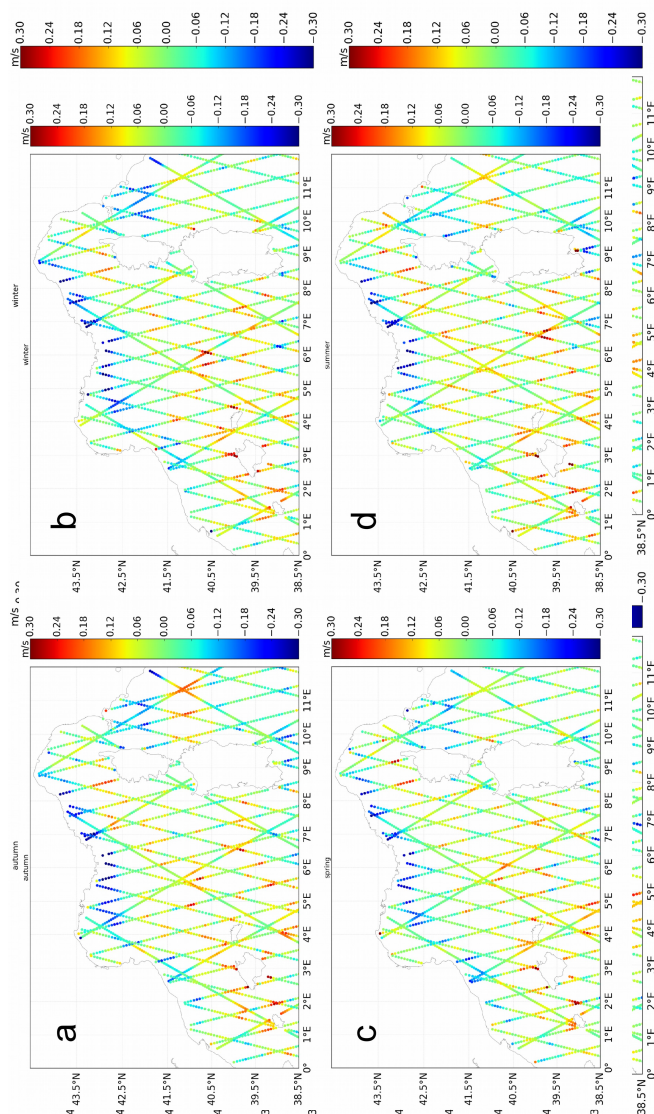
Figure 7: Seasonal climatology maps of cross-track geostrophic currents (in m/s) derived from Jason 2 and SARAL/AltiKa altimeter data over the period April 2013 – April 2016.